CHAPTER III

MÖSSBAUER SPECTROMETER

3.1 Introduction

The purpose of any Mössbauer spectrometer is to produce a known and precise small shift (approx. $1 : 10^{10}$ to $1 : 10^{14}$) in the energy levels of a nucleus located in the source and an isomer nucleus located in the absorber. This can be achieved by several means. The standard procedure is to produce a Doppler shift by a relative motion between source and absorber (velocity spectrometers).

Velocity spectrometers are of two basic types.

1) Constant velocity spectrometers : Either the source (or absorber) is moved with constant speed back and forth and this speed is changed step by step.

2) Constant acceleration spectrometers : The whole velocity range from $- V_{max} \longrightarrow 0 \longrightarrow + V_{max}$ is continuously swept through with a frequency typically between 1 and 100 Hz (velocity sweep spectrometer).

Both types can be based on mechanical or electromechanical designs. The latter are most widely used.

Constant velocity spectrometers have the advantage that an absolute velocity calibration can be carried out. This is true in particular for the mechanical types. In addition, constant velocity systems allow the experimenter to spend the measuring time predominantly in the velocity range of interest.

In velocity sweep spectrometers the count rate at various velocities within the range of interest is measured almost instantaneously. This eliminates the influence of slow fluctuation of the count rate due to drifts in the electronic pulse handling system or, with short-lived sources, to count rate changes during the experiment. They are, however, more costly to build since a multichannel analyzer (MCA), which sorts and stores the counts according to the instantaneous velocity, is required.

Three different types of velocity sweeps have found widespread acceptance. They are:

(a) Constant acceleration : The velocity is increased linearly from $- V_{max}$ through zero to $+ V_{max}$ and then decreased the same way back to $- V_{max}$. The sweep waveform is a symmetrical triangle.

(b) Constant acceleration with fly-back : The velocity is first increased linearly as described in (a), but then returned rapidly from $+ V_{max}$ to $- V_{max}$. The sweep waveform is a ramp. This however puts considerable stress on the transducer during the fly-back motion.

(c) Sinusoidal velocity sweep : The velocity is increased from $- V_{max}$ to $+ V_{max}$ sinusoidally and then decreased in the same fashion. The sweep waveform is a simple cosine and thus comes close to the natural frequency response of any oscillating system. Inertial forces are kept to a minimum.

Each of these waveforms has certain advantages and disadvantages, some of which will be discussed later. The basic electronic circuits, however, are similar and a well-designed transducer will follow any of these motions with high accuracy.

The spectrometer used in the present study is an electromechanical velocity sweep spectrometer with loudspeaker-type transducer. The block diagram of the electronic circuit used in this spectrometer is shown in Fig. 3.1.

The reference generator creates a triangular wave as a reference velocity sweep for the transducer. The transducer converts electrical signals into mechanical motion via the drive coil. The pick-up coil is mechanically connected to the drive coil and measures the instantaneous velocity of the motion. The negative feedback circuit, which consisted of an error amplifier (differential amplifier); a filter net work ; and a power amplifier, regulates the drive coil motion in such a way that its velocity sweep, as measured by the pick-up coil, follows exactly the output signal of the reference generator. Gamma rays emitted by the decay of a radioactive isotope are partially absorbed in an absorber containing the same isotope as the source. Some of the γ-rays pass through the absorber and are transformed into an electrical pulse proportional in height to the energy of the gamma ray detected in the detector. This analog pulse is then amplified by the spectroscopy amplifier. Part of the pulse spectrum is selected by a single channel analyzer (SCA) which in turn produces unit pulses. A MCA, operating in the multichannel scaling (MCS) or time mode, counts each pulse from the SCA in the channel which is open at that moment. A quartz-controlled pulse generator in the MCA opens one channel after the other at precisely constant time intervals. After addressing the last channel, a binary flip-flop in the analyzer address system switches from one set of memories to another set of equal

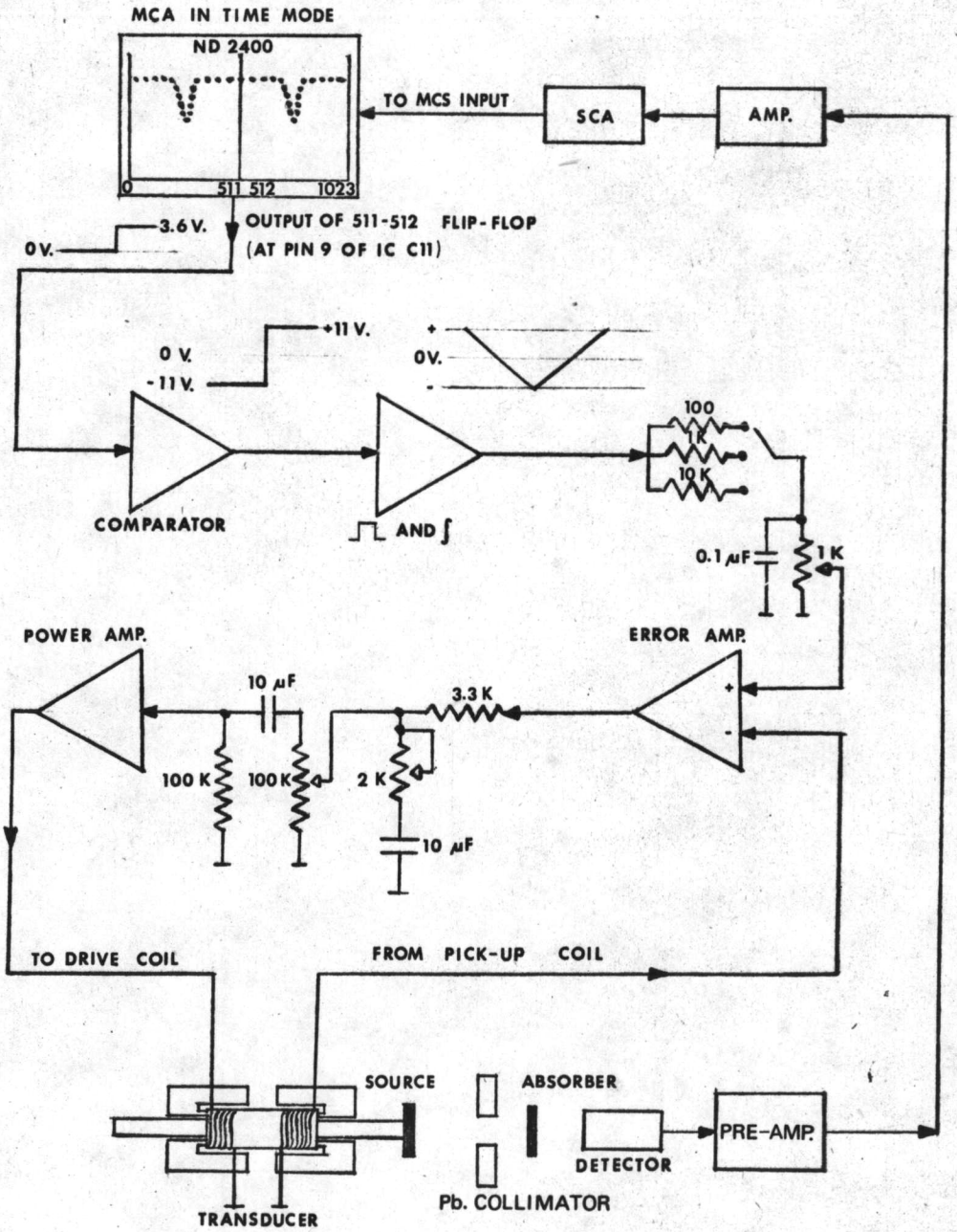

Fig. 3.1 Block diagram of the velocity spectrometer. (All resistance in ohm).

memories. In this manner, the repetitious scan through the channels is synchronized with the flip floping of the square wave d.c. signal. The square wave is then passed through the comparator circuit, in which a square wave a.c. signal can be obtained which is then modified by integration with the reference generator, constructed of IC-operational amplifiers, to produce a triangular wave. This signal can be produced with high precision. The time sweep of the MCS and the velocity sweep are in phase. Each channel number will correspond to a certain velocity interval. Two channels of the analyzer will therefore correspond to intervals of the same velocity. The CRT of the analyzer will display the velocity spectrum two times; the second half of the picture being the mirror of the first half.

3.2 Electromechanical Transducer (Loudspeaker-Type)

Figure 3.2 shows the design of the electromechanical transducer used in the present experiment, which is based on the transducer described by Kankeleit (1964). It consists of two loudspeaker-type systems rigidly connected front-to-front with brass bolts. Its moving parts include a drive and a pick-up coil both mounted on an aluminium rod connected to the frames of the loudspeakers by two linen - bakelite springs (1/32" thick). Their shape, as shown in Fig. 3.2, is chosen so that unwanted lateral or angular motion is reduced to a minimum. The pick-up and the drive coil are wound separately on the cylindrical paper at the ends of the connecting rod. The coils have a length of 0.25 in. The pick - up coil consists of 200 turns into four layers of 0.0036 - in. wire. The drive coil consists of 50 turns in two layers of bifilla type of 0.0068 - in. wire. The coils are free to move

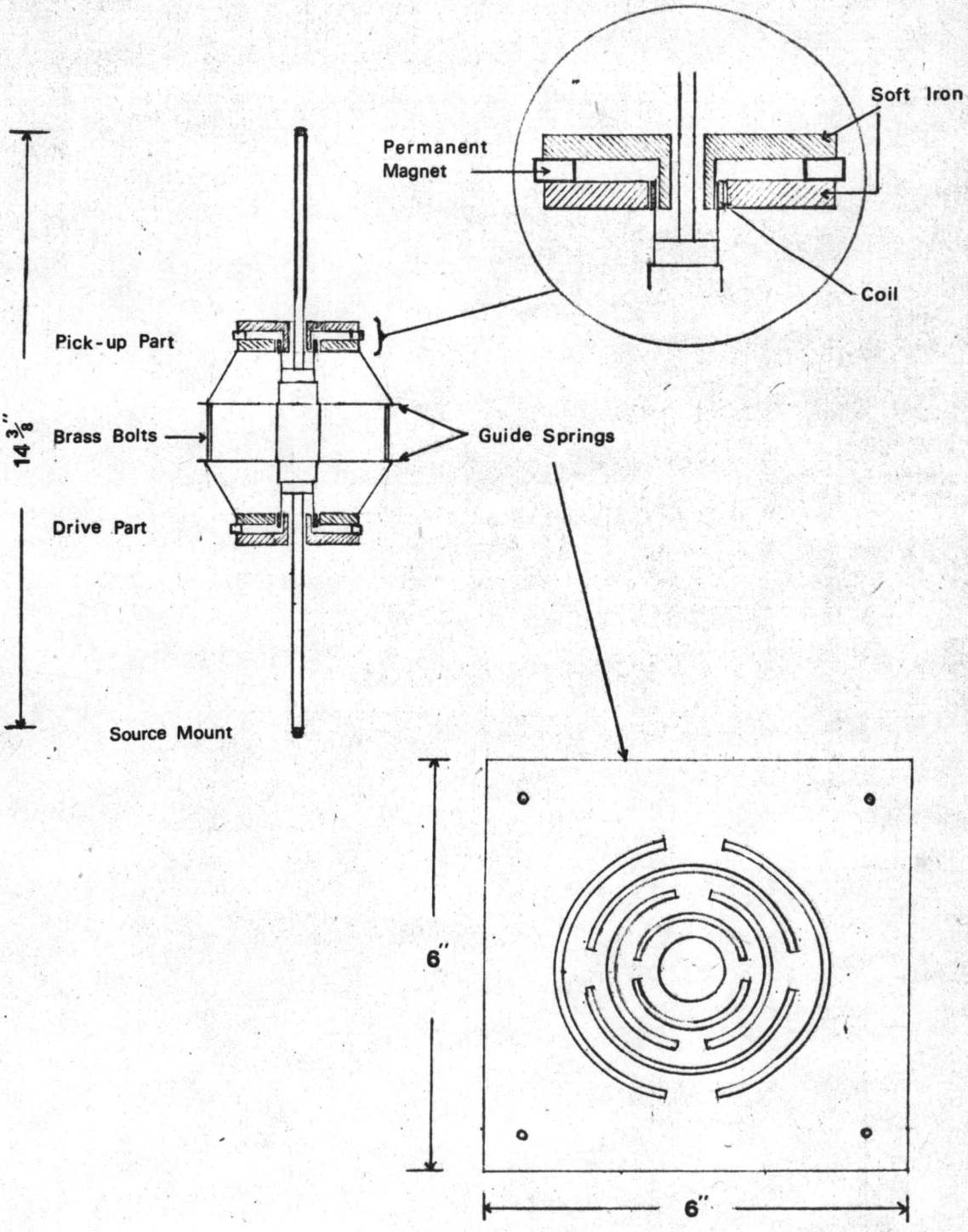

Fig. 3.2. Electromechanical transducer and the design of the guide spring.

in magnetic field gaps. The permanent magnets (10W "Bell") produce in the radial air gap a magnetic field of about 12 KG. The field was measured by a small Hall probe (Bell "120" Gauss Meter) in the axial direction. This system has the basic resonance frequency near 33 Hz for sinusoidal drive motion. The impedances of the drive coil and pick-up coil are 8.5 Ω and 512.5 Ω respectively at resonance frequency. The pick-up coil provides an output of approximately 150 mV for a velocity of 10 mm/sec, so that a voltage range of ± 150 mV is required on the velocity setting potentiometer to cover the range ± 10 mm/sec. For amplitudes of 0.1 mm (10 mm/sec at 25 Hz) the pick-up linearity is better than 0.15 %. It is likely that there is some asymmetry in the magnetic field between the inside and the outside part of the gap since the construction of the magnet system is not symmetric. These effects will cancel mostly if a symmetric sweep velocity waveform, such as a triangle, a sine, but not a ramp, is used and the data is then folded (see later in Chapter IV).

3.3 Reference Generator

The difference in the various means of creating the velocity sweep reference signal stems mainly from the problem of synchronizing the time sweep of the MCA to the velocity sweep. In general there are two possible ways of achieving synchronization :

1) the MCA time sweep is free running and the velocity signal is derived from the time sweep, or

2) the velocity signal generator is free running and controls

the MCA time sweep.

Both system have been refined to a high degree of perfection and one cannot recommend one particular design in preference to the other.

The method in 1), which has been used in the present study, has been described by Kankeleit (1964, 1965). The electronic circuits of the comparator and the reference generator are shown in Fig 3.3.

A square wave is initially produced by using the last bit of the binary address scaler (at pin 9 of IC C 11 of MCA ND 2400) which defines the first and the second half of the MCA memory. It is a d.c. signal (approx. 3.6 V), whose period depends on the number of channels of MCS used and the dwell time per channel selected. By using 1024 channels and 40 μs dwell time, the period is nearly equivalent to 24.4 Hz. The square wave derived by this method ensures symmetry of the period to a high degree. This guarantees that the magnitude of the slopes of the rising and falling part of the triangular wave are the same. This square wave can be modified by comparing it to a reference voltage at pin 4 (2.5 V) of IC_1, the comparator circuit, to produce a square wave a.c. signal at the frequency of the input signal. The square wave output voltage of the comparator is about 22 V_{p-p}. It is then passed through the squaring circuit consisting of I.C. operational amplifier type μA 741. The squaring circuit must also be free of hysteresis effects and be temperature stable. This can be achieved by a Zener diode clipping of the output of a high-gain, fast rising amplifier. The square wave obtained is then integrated further by the integrating circuit. The integrating stage should combine very good linearity with sufficient stability of

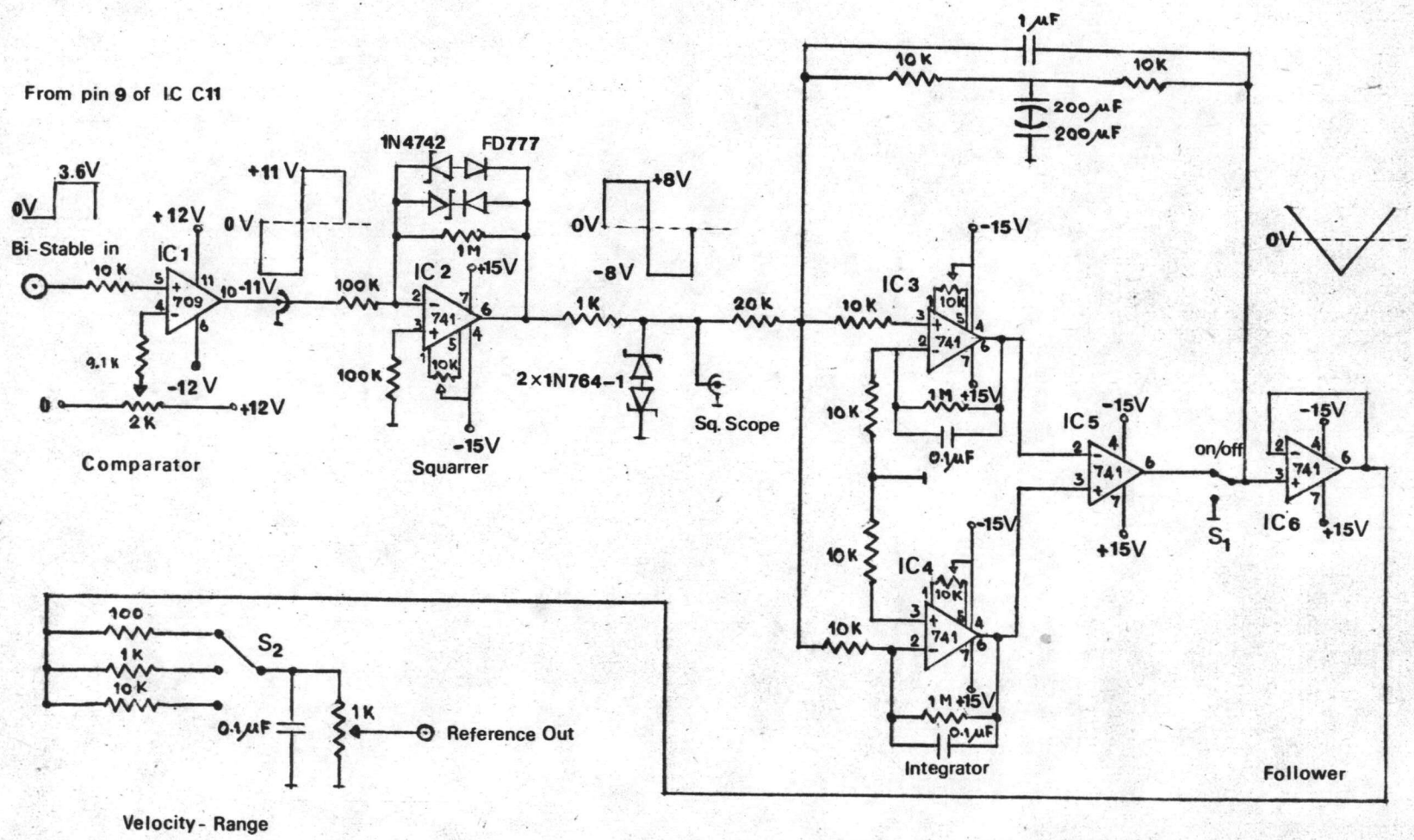

Fig. 3.3. The triangular wave reference generator and the comparator circuit.

(All resistance in ohm).

the output d.c. level. The difficulty in obtaining this is due to the fact that ideal integration is obtained with pure capacitive feedback of an operational amplifier, which means there is no d.c. level control possible. Therefore the drift of average voltage level about which the triangular wave swings, gives rise to a multitude of stability problems of the spectrometer. The design task is therefore to find an optimum compromise between d.c. feedback gain and triangle linearity. The integrating circuit shown in Fig. 3.3, the design was similar to that of Kalvius et.al. (1972), except a μA 727 operational amplifiers was replaced by the two μA 741 operational amplifiers and the d.c. off set was different. It was designed for a frequency of 25 Hz with a d.c. gain of about one. If another drive frequency is desired, the integrating capacitor (1 μF) should be appropriately adjusted. The integrating capacitor should be a high quality component and unpolarized. The 200 μF capacitors used are of the electrolytic type and mounted back-to-back. If the circuit of Fig. 3.3. is properly built with good quality components, a stable synchronized and highly linear triangular waveform will result, which then can be fed to the reference signal input of the feedback circuit.

Good amplitude stability is required of any waveform generator, it is therefore necessary to use a voltage follower as buffer to eliminate loading effect. The maximum sweep velocity should be selected by a twenty two turn potentiometer located at the Velocity-Range in Fig. 3.3. The capacitor 0.1 μF at the potentiometer is also of importance. (This will be discussed later).

3.4 Feedback System

It is the task of the electronic circuits to deliver a driving voltage that will produce the desired motion of the transducer. Knowing all pertinent parameters (like mass, spring constant, coil impedance, etc.) one can calculate the required shape of the driving voltage exactly. One would then have to build an appropriate wave generator to drive the transducer. Several papers dealing with this problem have appeared in the literature (Rubin, 1962 ; Zane, 1966 ; etc.). However it is of crucial importance to include a negative feedback loop in the drive circuit. This circuit compares the actual motion (as reflected in the pick-up signal) with the ideal velocity waveform (as presented by a reference waveform) and generates an appropriate correction signal (an error signal). If we make the feedback gain infinite, the feedback circuit by itself will deliver the appropriate drive waveform and separate reference waveform generator can be left out. As discussed by Kankeleit (1965), the presence of higher resonances in the electromechanical transducer limits the maximum allowable feedback gain. If a poor transducer is used, the limit on feedback gain will be low and the experimenter would be forced to use, in his drive unit, an externally generated correction signals (Zane, 1966). We have found that there is no need for this approach if proper care is taken in the mechanical and electronic design.

The feedback circuit consists basically of an error amplifier (differential amplifier), a filter network and a power amplifier. Without the network the system will fall into self-sustained oscillations

at a rather low overall feedback gain. A small second integration introduced into the feedback system (Cohen, 1963, and 1966) will improve the performance of some electromechanical transducers. Each transducer design will call for a slightly different time constant of the RC networks and optimization should be undertaken by the experimenter on a trial and error basis. A good feedback system will control the drive motion to a relative error $\frac{V_P - V_R}{V_R} \leqslant 10^{-3}$, for driving frequencies $\omega_o \leqslant \omega \leqslant 1.5\,\omega_o$ (Kalvius, et al., 1972). Here, V_P is the pick-up voltage, V_R the reference voltage, both measured peak-to-peak, and ω_o is the basic mechanical resonance frequency of the transducer.

Figure 3.4 shows the circuit of a feedback system using IC - operational amplifiers. By connecting the pick-up coil and the reference output of the circuit Fig. 3.3 at pins 4 and 5 via the 10 KΩ resistors of IC 7 respectively, the error signal is generated. IC 7 is an error amplifier constructed of μA 709 operational amplifier which is a differential amplifier having a gain of about 10. The error signal is fed through the variable low-pass filter and enters the power amplifier. The filter network consists of R_1, R_2 and C_2, the importance of which will be mentioned later. R_3 is the gain control of the feddback loop. C_4 and R_4 constitute a long time constant a.c. coupling to remove the d.c. component of the error signal from entering into a d.c. power amplifier. A driving d.c. power amplifier was designed to satisfy the following requirements : reliable response to very low input frequencies, sufficient output to supply power to the transducer. The first stage of the amplifier is the operational amplifier type μA 709 which provides

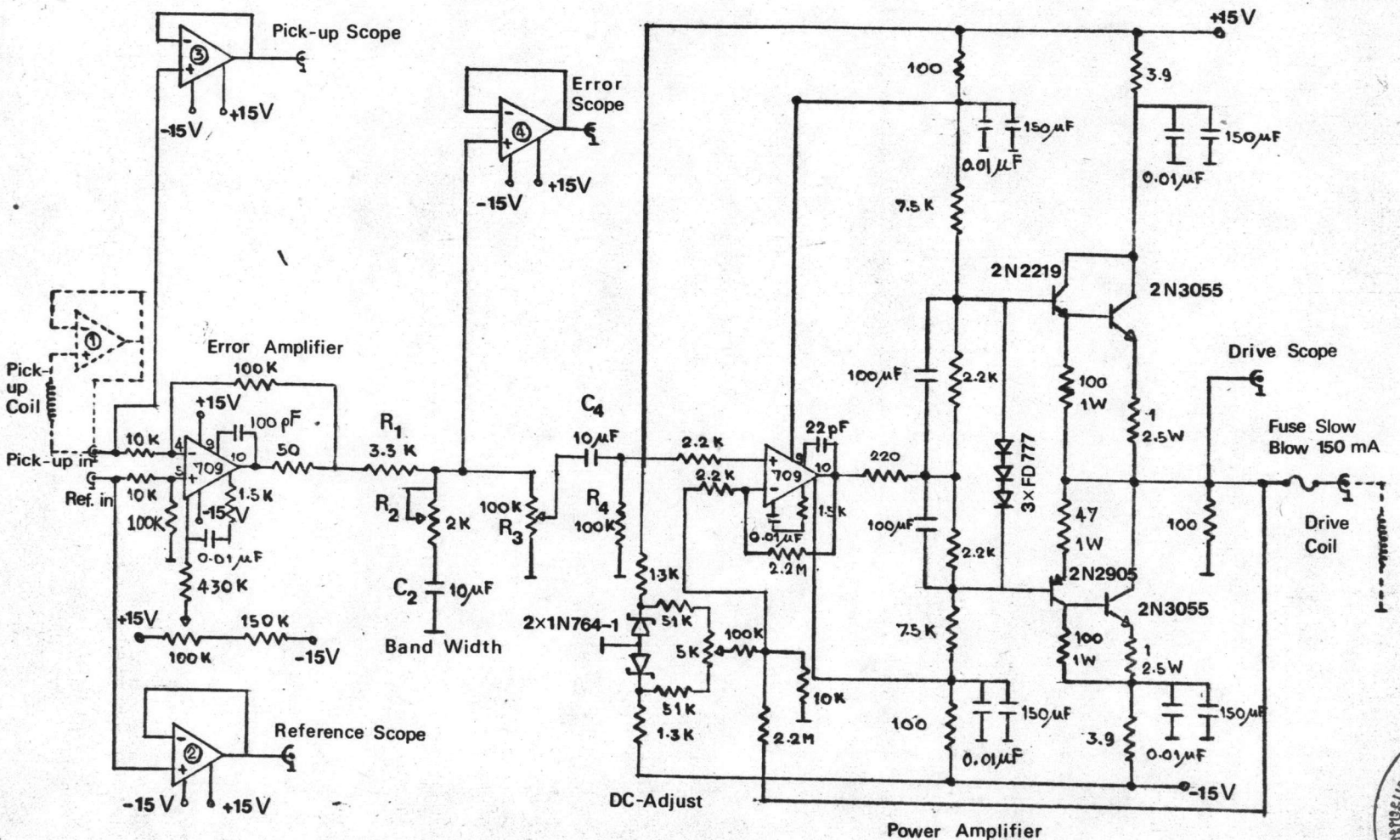

Fig. 3.4 . Circuit diagram of the feedback system. (All resistance in ohm).

the gain of the power amplifier. The final stage is a complementary Darlington connection of single-ended push-pull. A potentiometer 5 KΩ at the DC-Adjust position in Fig. 3.4 is used to balance the d.c. of the circuit. The operational amplifiers 1, 2, 3, and 4 are used as buffers to eliminate loading effects, the purpose of which is to see the waveforms that specified in the figure. In cases where long (> 10 m) cables are required between control electronics and Mössbauer drive (e.g. in an experiment involving a particle accelerator where one would like to have the electronics in the control room) it is best to use a voltage follower directly after the pick-up coil to reduce loading effects. This addition to the circuit is indicated by broken lines in Fig. 3.4.

3.5 Performance of the Feedback System

Now that the feedback system has been described, some merits of this velocity spectrometer will be summarized. Velocities in the range from 1 to 100 mm/sec can be controlled. The lower limit is determined by the amplifier input noise and the upper one by the elastic limitations of the springs and the uniform induction (over the amplitude driven) of the magnetic field in the gaps of the transducer. In the medium velocity range a linearity to a fraction of 0.5 % is possible.

These properties are possible to achieve because of the self-controlling features of the feedback system. Figure 3.4 shows that the feedback circuit consists of the error amplifier, the power amplifier with the RC network consisting of R_1, R_2, R_3, R_4, C_2 and C_4 between

them. The power amplifier drives the drive coil of the transducer which moves both the source of radiation and the pick-up coil, which in turn produces a signal proportional to the velocity. This voltage is subtracted from the reference signal at the error amplifier, thus producing the difference signal (error signal). The signal passes through the RC circuitry and re-enters the power amplifier so as to regulate the motion.

Figure 3.5 is a scheme of a control system which is commonly used by the control engineer.

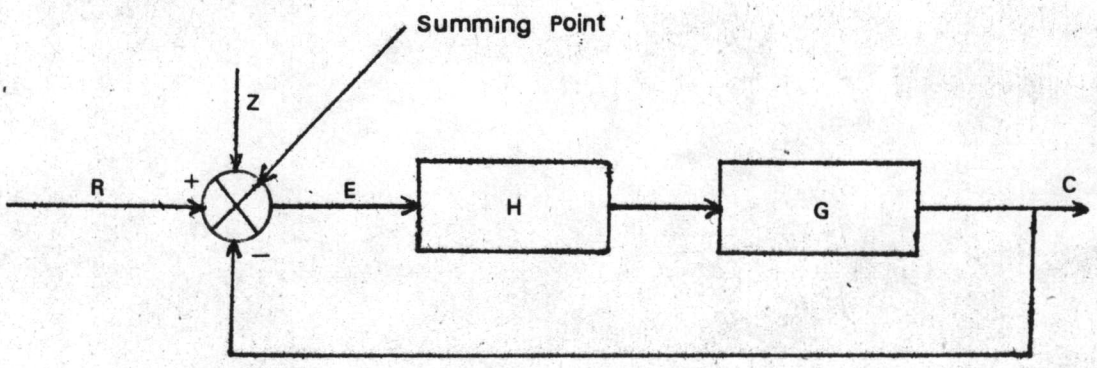

Fig. 3.5. A scheme of a control system.

The reference signal R, the triangular wave, is compared at the summing point with the so-called controlled variable C, the velocity pick-up signal. The difference, the error signal E, passes a frequency and phase-shaping unit H and is amplified by a factor G to produce the controlled variable C. While G is a number representing the gain

of the amplifier at the frequency with zero phase shift, those parameters of the system that affect its frequency and phase response are attributed to H. For our case, H includes the RC network, the high-frequency cut off of the amplifier, and the transfer response of the transducer. Therefore, H can be initially described only by a complicated set of integral and differential equations with respect to time. Application of Laplace transforms to these equations produces the following simple equations :

$$C = H \cdot G \cdot E = H \cdot G\,(R - C) \qquad (3.5.1),$$

$$\frac{R}{E} = 1 + H \cdot G \qquad (3.5.2),$$

$$\frac{C}{R} = 1 - \frac{1}{1 + H \cdot G} \qquad (3.5.3).$$

We can see from eq. (3.5.3) that for $H \cdot G >> 1$, $\frac{C}{R} = 1$, i.e., the controlled variable C will be equal to the reference signal R. We can also see that the properties of H do not enter the ratio C/R.

Some disturbances Z (for instance, 50 Hz noise, seismic vibration) acting on the system that produce spurious amplifier outputs, can have their effects drastically reduced. Generally, we will see that Z is very small with respect to R.

It is very unfortunate that the product G.H can not be made to be infinite. In our system we will observe that increasing the gain beyond a certain point will cause the system to oscillate at high

frequencies. The instability is caused by the fact that the function H, generally a complex function, can become a real negative quantity. At certain values of G the product H·G can approach -1, and according to eq. (3.5.3), C/R becomes infinite. In other words, H shifts the phase by 180° and therefore we have positive feedback, a condition employed for oscillators.

The most important source of the phase shift is the transducer itself. In Fig. 3.6, a so-called Nyquist diagram for the transducer, as shown in Fig. 3.2, is sketched. This diagram has been obtained by the following procedure. A sine-wave oscillator was connected to the drive coil via a 1 ohm resistor. The input current was calculated by measuring the voltage drop across this resistor with an oscilloscope. The pick-up voltage of the transducer was calculated and displayed with a second scope trace. The phase shift between the two sine waves is drawn as an angle between a vector from the origin and the real axis in the Nyquist diagram. A positive angle means phase leading of the pick-up voltage with respect to the input current. The length of the vector is the ratio of pick-up voltage amplitude to input current amplitude. Plotting this as a function of frequency, we obtain a curve which starts from the point (1.4, + 97.2) at the frequency about 10 Hz. For frequencies less than 10 Hz, the transducer does not respond to vibration at the frequency of the input sine wave. At 25 Hz, the curve cuts the imaginary axis and bends off into an approximate circle. However, a zero phase shift at 27.5 Hz that deforms the curve from what it should be, is probably due to a basic resonance oscillation of the bakelite springs. We observe a maximum of the amplitude ratio at 33.3 Hz, the main resonance,

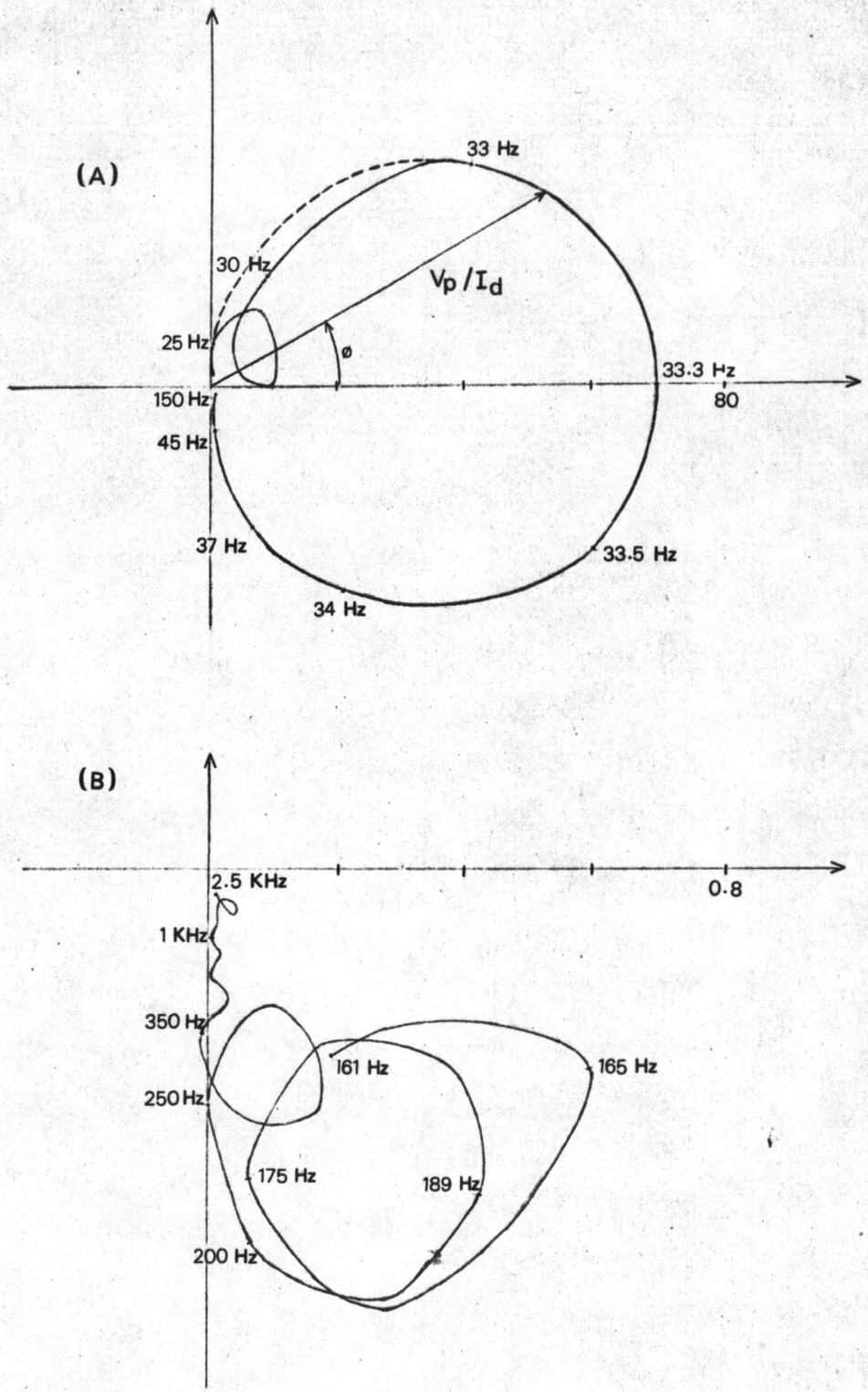

Fig. 3.6 Nyquist diagram of the transducer.

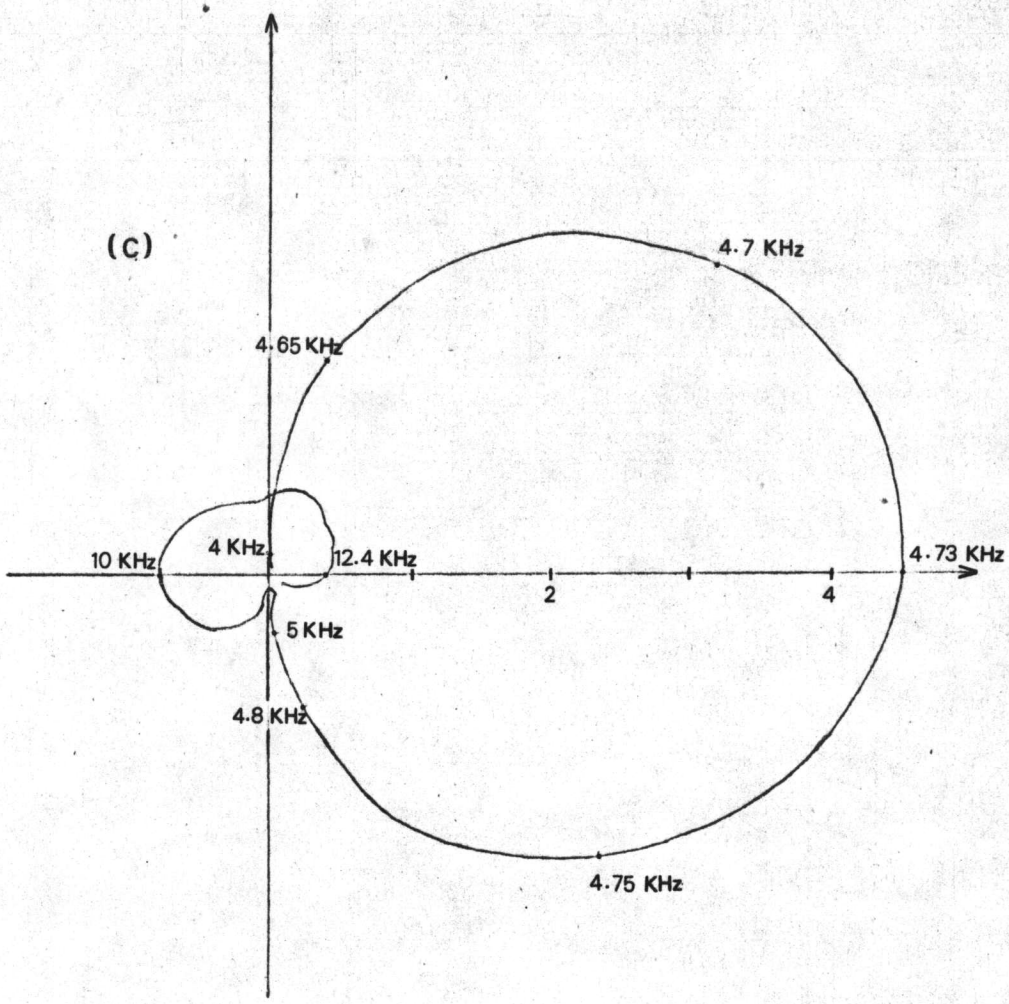

Fig. 3.6. Nyquist diagram of the transducer.

at zero phase angle. At much higher frequencies, resonance oscillations, probably in the aluminium rod connecting the drive and pick-up coil, appear. The negative null axis is crossed at 10 KHz. A phase shift of 180° is therefore contributed by the transducer itself. It is obviously necessary that $H \cdot G$ be optimized. Thus, the design for the structure of the transducer is extremly important. A very rigid connection between the two coils is essential. It will minimize the effects of high-frequency vibrations by shifting them to higher frequencies.

We now study the behaviour of the function $H \cdot G$ for the transducer by looking at the absolute ratio $|R/E| = |1 + H \cdot G|$ of the eq. (5.3.2) only. Therefore, we use the feedback circuit of Fig. 3.4 but remove the capacitor C_2. As a reference signal R we again use a sine wave. In Fig. 3.7. the ratio $|R/E|$ is plotted as a function of frequency. The gain was set slightly below the onset of oscillation. The lower curve of Fig. 3.7 shows that only a rather low value of amplifier gain is permissible. At the resonance frequencies of 28 Hz and 34 Hz the maximum gains are only 50 and 80 respectively corresponded to the nature of the transducer. At lower and higher frequencies the gain rapidly drop off.

An improvement is gained by the insertion of the integrating capacitor C_2. Varying R_3, the loop gain control, and R_2, the phase lag control, we are able to increase the gain by a large factor. The upper curve of Fig. 3.7 shows the frequency response curve under optimum condition. At the main resonance the gain is now 2500.

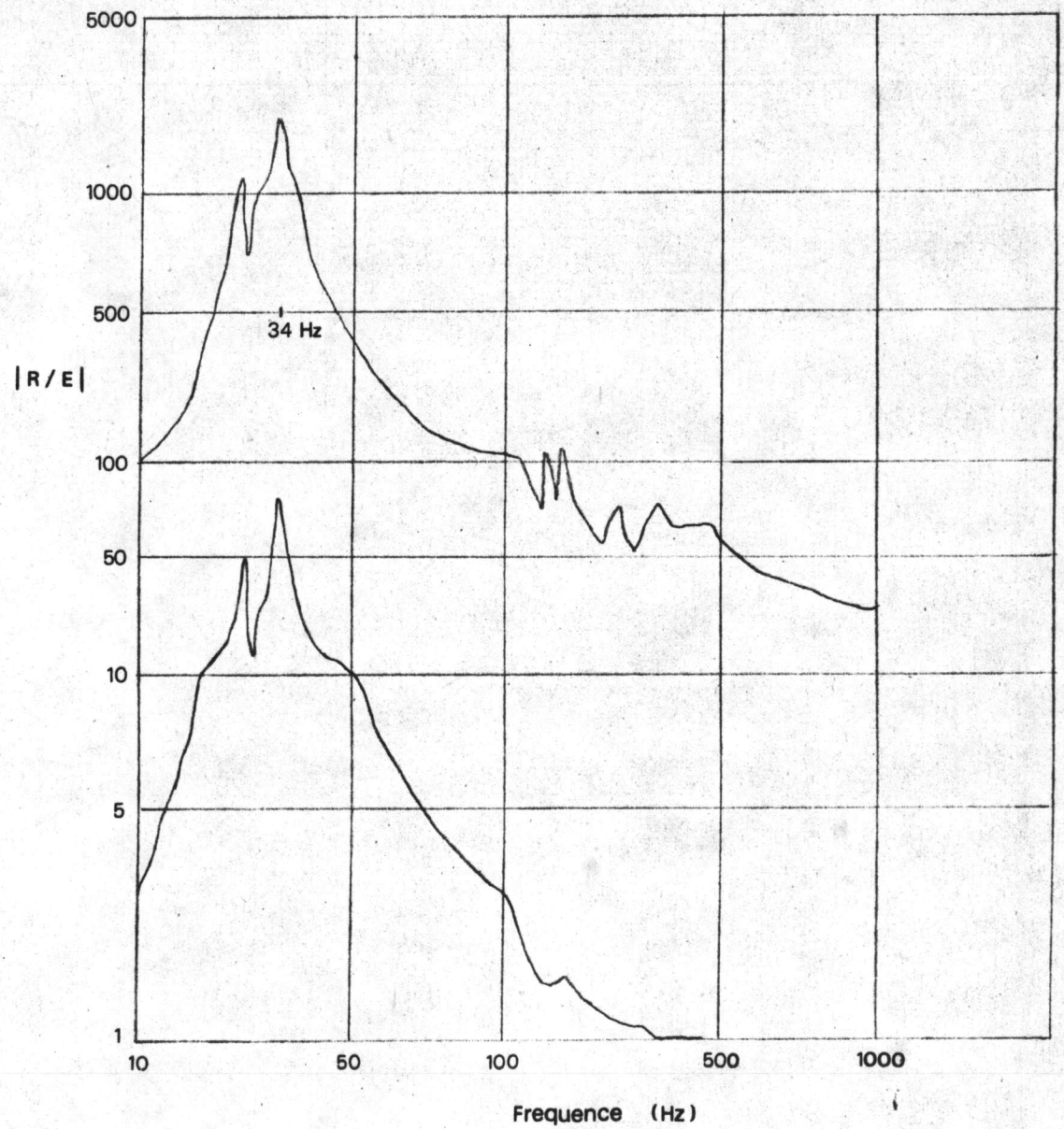

Fig. 3.7 Frequency response curve |R/E| with (upper curve) and without integration (lower curve).

The reason for this improvement is due to the damping action of capacitor C_2 on the above-mentioned high frequencies. However the selection of capacitor C_2 and R_2 is rather critical. The resistor R_2 actually reduces the effect of the capacitor C_2 at very high frequencies (integrator with stop). The point is that the integrating capacitor unavoidably introduces phase lagging shifts. In the Nyquist diagram of Fig. 3.6, the inclusion of the R_2C_2 network would mean that the high-frequency part would be shifted toward larger negative angles. Thus at lower frequencies a crossing of the negative real axis results, while on the other hand, the high-frequency amplitudes are decreased and moved toward the origin.

At this point, a short remark about the capacitor C_4 in Fig. 3.4 is in order. This capacitor eliminates the above mentioned shift problem due to the integrating operational amplifiers. It also affects the low-frequency part of the Nyquist diagram in that the curve would shift to larger phase leading angles and if there are more than one RC coupling the curve would start at the negative imaginary axis at very low frequencies. Then the feedback system can again start an oscillatory instability at low frequency when the curve is crossing the negative real axis ($+ 180^{\circ}$). The point is that only one differentiating network is allowed.